PALEOMAP Paleodigital Elevation Models (PaleoDEMS) for the Phanerozoic

by

Christopher R. Scotese

Department of Earth & Planetary Sciences, Northwestern University, Evanston, 60202

cscotese @ gmail.com

and

Nicky Wright

Research School of Earth Sciences, Australian National University

nicky.wright@anu.edu.au

August 1, 2018

Abstract

A paleo-digital elevation model (paleoDEM) is a digital representation of paleotopography and paleobathymetry that has been "reconstructed" back in time. This report describes how the 117 PALEOMAP paleoDEMS (see Supplementary Materials) were made and how they can be used to produce detailed paleogeographic maps. The geological time interval and the age of each paleoDEM is listed in Table 1. The paleoDEMS describe the changing distribution of deep oceans, shallow seas, lowlands, and mountainous regions during the last 540 million years (myr) at 5 myr intervals. Each paleoDEM is an estimate of the elevation of the land surface and depth of the ocean basins measured in meters (m) at a resolution of 1x1 degrees. The paleoDEMs are available in two formats: (1) a simple text file that lists the latitude, longitude and elevation of each grid point; and (2) as a netcdf file. The paleoDEMs have been used to produce: a set of paleogeographic maps for the Phanerozoic, a simulation of the Earth’s past climate and paleoceanography, animations of the paleogeographic history of the world’s oceans and continents, and an estimate of the changing area of land, mountains, shallow seas, and deep oceans through time. A complete set of the PALEOMAP PaleoDEMs can be downloaded at https://www.earthbyte.org/paleodem-resource-scotese-and-wright-2018/.

Introduction

The paleoDEMS described in this report were produced by C.R. Scotese as part of the research work of the PALEOMAP Project (2003–2013). In 2017, Nicky Wright converted the text file versions of the paleoDEMS into netcdf files.

Please cite this work as: Scotese, C.R., and Wright, N., 2018. PALEOMAP Paleodigital Elevation Models (PaleoDEMS) for the Phanerozoic PALEOMAP Project, https://www.earthbyte.org/paleodem-resource-scotese-and-wright-2018/

The paleoDEMs were used to produce the 120 paleogeographic reconstructions (117 Phanerozoic and 3 Precambrian) that make up the PALEOMAP Paleogeographic Atlas (Figure 1, Table 1). These paleoDEMs were produced in two phases:

1. Phase I (2003–2008): 50 paleoDEMS were constructed for the time intervals indicated in **bold** type in Table 1 (Scotese, 2008a-f).
2. Phase II (2010–2013): paleoDEMs for the intervening time intervals were produced so that paleogeographic maps could be constructed at 5 myr intervals throughout the Phanerozoic (Table 1; Scotese, 2014m-r).

These interpolated paleoDEMs from Phase II guaranteed that there would be a paleogeographic map for every stage in the Phanerozoic. Multiple paleoDEMs were made for some especially long geologic stages (i.e., Campanian, Albian, Aptian, and Norian, Carnian, Kungurian, Visean, Tournaisian, Famenian, Frasnian, Emsian, Llandovery, Darwillian, and Terreneuvian). Additional paleogeographic maps were produced representing important sequence stratigraphic events such as highstand maximum flooding surfaces or lowstand sequence boundaries.

From 2008 to 2013, 22 of the paleoDEMS were used as boundary conditions for paleoclimate simulations using the FOAM climate model (Moore and Scotese, 2010), as part of the GANDOLPH Project (Scotese et al., 2007, 2008, 2009, 2011). A list of the time intervals for which paleoclimate simulations were run is given in Figure 2 (Moore and Scotese, 2010). The various paleoclimatic and paleoceanographic reconstructions that were produced for the GANDOLPH Project and the PALEOMAP PaleoAtlas (Scotese, 20014, m-r) is given in Figure 3. These maps illustrate global paleotemperature (Scotese and Moore, 2014c), paleo-winds and atmospheric pressure (Scotese and Moore, 2014d), paleo-rainfall and runoff (Scotese and Moore, 2014b), paleosalinity of the oceans (Scotese and Moore, 2014a), paleo-surface currents (summer and winter) (Scotese and Moore, 2014a), regions of paleo-anoxia (Scotese, 2014a), and zones of paleo-upwelling (Scotese and Moore, 2014e). The legend for these paleoclimatic reconstructions is given in Figure 4.

In addition to these paleoclimatic and paleoceanographic reconstructions, the paleoDEMS were used as the basemaps for an atlas of plate tectonic reconstructions that illustrates the past locations of mid-ocean ridges, subduction zones, major strike-slip faults, continental volcanic arcs, and collision zones (Scotese, 2014b). The paleoDEMS were also used to estimate the changing area of continental and oceanic lithosphere, the degree of continental flooding, and the area of mountainous regions through time (Scotese et al., 2016a). In short, the paleoDEMS are the foundation upon which the research synthesis that defines the PALEOMAP Project rests.

You are welcome to freely use the 1° x 1° paleoDEMS for your own research projects, presentations, and publications. If you have any questions, please contact C.R. Scotese at cscotese@gmail.com.

How the PaleoDEMS were Made: The Paleogeographic Method

In this section, I briefly discuss the geologic and geophysical data that were used to make the PaleoDEMS and describe the methodology that was followed to reimagine the paleotopography and paleobathymetry, (i.e. the paleogeography).

The paleogeographic maps of the PALEOMAP PaleoAtlas were originally published in the PALEOMAP PaleoAtlas for ArcGIS (Scotese, 2008a-f; Scotese, 2014m-r). This digital atlas, designed for use with GIS software (e.g., ESRI ArcMap), consists of 120 paleogeographic maps together with plate tectonic (Scotese, 2014bh), paleolithological (Boucot et al., 2013; Scotese et al., 2014), paleoceanographic (Scotese, 2014a; Scotese and Moore, 2014a,e), and paleoclimatic reconstructions (Moore and Scotese, 2010; Scotese and Moore, 2014b,c,d).

Once a global plate tectonic framework had been established (Scotese and Sager, 1988; Scotese, 1990; Scotese and McKerrow, 1990; Scotese, 2001; Scotese and Dammrose, 2008; Scotese, 2014h, 2015, 2016b, 2017; Scotese and Elling, 2017), paleogeographic maps that represent the ancient distribution of highlands, lowlands, shallow seas, and deep ocean basins were be digitally constructed. This was done in several steps. The first step was to map the geological lithofacies that defined the ancient depositional environments (Figure 5). For example, a thick sequence of pure limestones might represent warm, shallow water environments like the Bahamas Platform or vast a epeiric sea. Extensive sets of massive, cross-bedded sandstones may once have been wind-blown, desert dunes. A terrane composed of andesite and granodiorite may have been a continental arc or Andean mountain range. Table 2 summarizes the lithofacies and rock types that correspond to the depositional environments that have been used to interpret the ancient topography and bathymetry.

Geologists have been collecting lithologic information and producing lithofacies and paleoenvironmental maps for more than 20 years (William Smith, 1815). During the late 1970's and early 1980's, the Paleogeographic Atlas Project, under the leadership of Prof. A. M. Ziegler, in the Department of Geophysical Sciences, University of Chicago, compiled a database of more than 125,000 lithological and paleoenvironmental records for the Mesozoic and Cenozoic (Ziegler, 1975; Ziegler and Scotese, 1977; Ziegler et al., 1985). This database was supplemented by additional lithological and paleoenvironmental records for the Permian and Jurassic (Rees et al., 2000; 2002). These two datasets, in combination with numerous regional and global paleogeographic atlases, were used to construct the paleogeographic maps that appear in the PALEOMAP PaleoAtlas.

Lithofacies can be used to map paleogeographic environments where only the rock record is fairly complete. However, there are many instances where the rock record has been eroded, destroyed by tectonic processes, or covered by younger strata. For these areas, a second, more interpretive approach needs to be taken to restore the paleogeography. In these instances, the paleoenvironments and paleogeography must be inferred from the tectonic history of a region. The PALEOMAP Global Plate

Tectonic Model (Scotese, 2016b), provided the tectonic framework required to make these inferences and interpretations. The plate tectonic reconstructions (Scotese, 2014b, 2015, 2017; Scotese and Elling, 2017) were used to “model” the expected changes in topography and bathymetry caused by plate tectonic events, such as: sea floor spreading, continental rifting, subduction along Andean margins, and continental collision, as well as other isostatic events such as glacial rebound (Peltier, 2004). For example, to produce a paleogeographic map for the early Cretaceous, young tectonic features such as recent uplifts or volcanic eruptions (e.g. Mid-African Rift), must be removed or reduced in size whereas older tectonic features such as ancient mountain ranges (e.g. Appalachian mountians) must be restored to their former extent. This approach is similar to the techniques described by Vérard et al. (2015) and Baatsen et al. (2015).

In a similar manner, the paleobathymetry of the ocean floor must be restored back through time. Oceanic lithosphere is produced at mid-ocean ridges, and as ocean floor moves away from the spreading ridge, it cools and subsides. In many respects restoring the past bathymetry of the ocean floor is much easier than estimating the elevation of ancient mountain ranges (Rowley et al., 2001; 2006; 2007). This is because as the ocean floor ages, it cools, and as it cools, it sinks. The amount that it sinks through time follows a regular mathematical rule that states that the amount of thermal subsidence is inversely proportional to the square root of the age of the oceanic crust (Parsons and Sclater, 1977). To restore the ancient ocean floor to its former depths, the bathymetry of the ocean floor was “unsubsided” using the depth/age relationship published by Stein and Stein (1992).

Once the paleogeography for each time interval was mapped and the corrections to the topography and bathymetry have been duly noted, this information was then converted into a digital representation of paleotopography and paleobathymetry (i.e. PaleoDEM). Each high resolution paleoDEM is composed of over 6 million grid cells that capture digital elevation information at a 10 km x 10 km horizontal resolution and 40 m vertical resolution. This quantitative, paleo-digital elevation model allows us to visualize and analyze the changing surface of the Earth through time using GIS software and other computer modeling techniques. A low resolution, 1° x 1° grid of paleoelevations suitable for paleoclimate modeling is provided with this report (see Supplementary Materials). The higher resolution paleoDEMS (0.1° x 0.1°) are not included in the Supplementary Materials, but can be made available upon request.

The process of building a paleoDEM (Scotese, 2002) begins with the digital topographic and bathymetric data sets of the modern world (Smith and Sandwell, 1997), Antarctica (Lythe and Vaughan, 2000), and the Arctic, (Jakobsson et al., 2004). These topographic and bathymetric data sets are combined into a global data set with 6-minute resolution. In the next step, the individual grid cells (latitude, longitude) are rotated back to their paleopositions using the global plate tectonic model of the PALEOMAP Project (Scotese, 2015, 2016b; Scotese and Elling, 2017). The resulting map is a reconstruction of present-day bathymetry and topography in a paleolatitudinal and paleolongitudal framework.

In the next processing steps (Scotese, 2002), the modern digital topographic and bathymetric values are corrected and modified using the lithofacies and paleoenvironmental information described in the previous section. This is done using modern analogs for ancient geographies and simple computer graphics techniques. In this step, the digital elevation information is converted to “grayscale” values, where white (grayscale value = 255) represents the highest elevations (+10,000 m) and black (grayscale value=0) represents the deepest ocean trenches (-10,000 m). Using 256 grayscale values it is possible to map the topography and bathymetry at a resolution of 40 m, vertically. There are fewer grayscale values for high mountains and deep trenches because these regions represent only a small portion of the Earth's surface.

To increase or decrease the elevation of a pixel, it becomes simply a matter of changing the grayscale values until the digital model matches the paleoenvironment or a modern analog. For example, the modern topography for the East African Rift was produced during the last 30 myr. Therefore, on a late Eocene (35 Ma) paleogeographic map of East Africa, the modern topography of the East African Rift must be "erased". This was accomplished by digitally editing the mountainous grayscale values and replacing them with the grayscale values that represent lowlands and plains. Conversely, an area that was once was an ancient rift valley, but has been eroded flat, was "rejuvenated" by replacing them with grayscale values that represent highlands. A reasonable way to do this is to use the modern topography as an analog. For example, the detailed "continental rift" topography in the proto-South Atlantic region shown in Figure 1, was actually "cloned" from portions of the East African Rift.

In either case, recreating ancient topographic features requires a thorough understanding of the overall tectonic evolution of a region, as well as the precise knowledge of the tectonic history of every important geographic feature. One must be able to answer questions like: "When did this geographic feature first appear?", "How long did it remain an important geographic feature?", "When was it eroded?". It is also important to note that any changes made on one map must be consistent with the preceding map, as well as, with subsequent paleogeographies. That is to say, tectonic features don't suddenly appear and disappear. In fact the best overall strategy, when building the paleotopographic models, is to start at the present-day geography and work systematically backwards though time, map by map, undoing most recent tectonic events and gradually recreating ancient tectonic features.

Continuing with our discussion of the methodology used to produce the paleoDEMS, once the grayscale version of the paleoelevations has been completed, then the grayscale values can be converted back to digitial elevation values. The resulting digital elevation file is a "revised" global paleotopographic and paleobathymetric surface, or paleoDEM, that represents the elevation of the land surface and the depth of the ocean basins for a specific geological time interval.

The final step in the process is the simplest, but the most dramatic. A paleogeographic map can now be produced by giving eah grid-cell in the paleo-digitial elevation model (PaleoDEM) a unique color based on its depth or elevation (Figure 1). Deep oceans (oceanic crust) - dark blue. Mid-ocean ridges - blue. The shallow shelves and the flooded portions of the continents (epeiric seas) - shades of light blue. Coastal regions and continental areas near sea level - dark green; low-lying inland areas - green. Plateaus and the foothills of mountains - tan, and mountainous regions - brown. The highest peaks in the mountains - shaded white (Figure 6). The resulting paleogeographic map is the "best guess" or average paleogeography for the time interval represented by the paleoDEM (Figure 7B).

It is possible to produce multiple paleogeographic maps from the same paleoDEM. For example, a transgressive or "highstand" paleogeography can be visualized by digitally "flooding" the topography

(Figure 7A). Conversely, a regressive or “lowstand” paleogeography can be visualized by digitally lowering sea level (Figure 7C).

A complete set of the highstand/lowstand paleogeographies can be viewed in the accompanying paleogeographic atlases (Scotese, 2014c-1; Supplementary Materials). As a consequence of this analysis, we have found that the most widely used estimates of sea level are either too high (Haq et al., 1987; Haq and Schutter, 2009) or too low (Miller et al. (2005). If the Haq and Schutter (2009) estimates of sea level are reduced by 30-40%, there is a better match between predicted area of continental flooding and the geological evidence regarding the extent of ancient shallow seas.

Discussion & Future Developments

The paleoDEMS provided with this report are a “first draft”. Corrections and improvements need to be made, including: (1) estimates of the paleobathymetry of subducted ocean floor; (2) revised estimates of the paleobathymetry of the deep ocean for the Paleozoic; (3) correction to errors in paleotopography; (4) update to the location of paleoshorelines; and (5) update to the estimates of highstand shorelines (maximum flooding surfaces) and lowstand shorelines (major sequence boundaries).

Using Pacific isochrons, it is possible to recreate the conjugate isochrons of the Farallon, Kula, Izanagi, and Phoenix plates that have been subducted (Scotese, 2017). These synthetic isochrons cane be used to estimate the age of the ocean floor back to ~200 million years. Knowing the likely age of subducted ocean floor, it is then possible to estimate the paleobathymetry.

Reconstructing the bathymetry of Paleozoic ocean floor has been especially challenging. Except for minor ophiolites, all the ocean floor of Paleozoic age has been subducted. In the paleoDEM models presented here the depth of the deep, Paleozoic ocean basins has been fixed at a depth of 4800 m. This is substantial shallower than the average depth of the modern deep ocean basins (5400 m). An average depth of 4800 m is required to conserve the volume of the water in the ocean basins. It may be possible to make a better estimate of paleobathymetry of the Paleozoic ocean basins by including the location of Paleozoic spreading centers and subduction zones (Scotese, 2017).

There are numerous errors in the paleotopography. Often young topographic features appear on older maps. Some geographic features appear, disappear, then reappear. In addition, the height of the highest mountain ranges is likely overestimated. It may be possible to improve the topographic estimates if simplifying assumptions are made regarding the hypsometry of upland areas through time. Also, a stipulation that the Earth’s mean radius must not change (Rowley, 2017), may also help to constrain both bathymetric and topographic estimates.

In the next version of the paleoDEMs additional lithologic data will be brought to bear to help locate “lowstand shorelines” and “highstand shorelines”. This data includes information from the Paleogeographic Atlas Project (Ziegler et al., 1985), the Paleobiology Database (Alroy, 2003), and the Atlas of Paleoclimate (Boucot et al.,2013). See Wright et al. (2013), Scotese and Schettino (2017) and Cao et al. (2017) for descriptions of this methodology.

In the next version of the paleoDEM grids, we will be making available a complete set of paleoDEMS at an intermediate resolution (0.5° x 0.5°). Please feel free to contact me with comments or questions at: cscotese@gmail.com.

Please cite this work as: Scotese, C.R., and Wright, N., 2018. PALEOMAP Paleodigital Elevation Models (PaleoDEMS) for the Phaerozoic PALEOMAP Project, https://www.earthbyte.org/paleodem-resource-scotese-and-wright-2018/

References

Alroy, J., 2003. Patterns of ecological dominance throughout the fossil record: A demonstration of the Paleobiology Database, (abstract), Paper No. 177-2, Geological Society of America Annual Meeting, November 2-5, 2003, Seattle, WA.

Baatsen, M., van Hinsbergen, D.J.J., von der Heydt, A.S., Dijkstra, H.A., Sluijs, A., Abels, H.A., and Bijl, P.K., 2015. A generalized approach for reconstructing geographical boundary conditions for palaeoclimate modeling, Climate of the Past Discussions, v. 11, p. 4917-4942.

Boucot, A.J., Chen Xu, and Scotese, C.R, 2013. Phanerozoic Paleoclimate: An Atlas of Lithologic Indicators of Climate, SEPM Concepts in Sedimentology and Paleontology, (Print-on-Demand Version), No. 11, 478 pp., ISBN 978-1-56576-289-3, October 2013, Society for Sedimentary Geology, Tulsa, OK.

Cao, W., Zahirovic, S., Flament, N., Williams, S., Golonka, J., and Müller, R.D., 2017. Improving global paleogeography since the late Paleozoic using paleobiology, Biogeosciences, v. 14, p.5425-5439.

Haq, B. U., Hardenbol, J., and Vail, P.R., 1987. Chronology of Fluctuating Sea Levels Since the Triassic, Science, v. 235, p. 1156-1167.

Haq, B.U., and Schutter, S. R., 2009. A Chronology of Paleozoic Sea-Level Changes, Science, v. 322, p. 64-68.

Jakobsson, M., MacNab, R., Cherkis, N., and Schenke, H-W, 2004. The International Bathymetric Chart of the Arctic Ocean (IBCAO), Research Publication RP-2, National Geophysical Data Center, Boulder, CO.

Lythe, M.B., Vaughan, D.G., and the BEDMAP Consortium, 2000. BEDMAP: Bed Topography of the Antarctic, Misc. 9, scale 1:10,000,000, British Antarctic Survey, Cambridge, U.K.

Miller, K.G., Kominz, M.A., Browning, J.V., Wright, J.D., Mountain, G.S., Katz, M.E., Sugarman, P.J., Cramer, B.S., Christie-Blick, N., and Pekar, S.F., 2005. The Phanerozoic Record of Global Sea-Level Change, Science, v. 310, p. 1293-1298.

Moore, T.L., and C.R. Scotese, 2010. The Paleoclimate Atlas (ArcGIS), Geological Society of America, 2010 Annual Meeting, Abstracts with Programs, 42:598.

Ogg, J.G., Ogg, G, and Gradstein, F.M., 2008. The Concise Geologic Time Scale, Cambridge University Press, 177 pp.

Parsons, B. and Sclater, J.G., 1977, An analysis of the variation of ocean floor bathymetry and heat flow with age, Journal of Geophysical Research, v. 82, no. 5, p. 803-827.

Peltier, W.R., 2004. Global Glacial Isostasy and the Surface of the Ice-Age Earth: The ICE-5G (VM2) Model and GRACE, Annual Review of Earth and Planetary Sciences, v. 32, p. 111-149.

Rees, P.M., Ziegler, A.M., Gibbs, M.T., Kutzbach, J.E., Behling, P., and Rowley, D.B., 2002. Permian phytogeographic patterns and climate data/model comparisons, Journal of Geology, v. 110, p. 1-31.

Rees, P.M., Ziegler, A.M., and Valdes, P.J., 2000. Jurassic phytogeography and climates: new data and model comparisons, in B.T. Huber, K.G. Macleod, and S.L. Wing (editors), Warm Climates in Earth History, Cambridge University Press, p. 297-318.

Ross, C.A., and Ross, J.R.P., 1985. Late Paleozoic depositional Sequences are synchronous and worldwide, Geology, (March), v. 13, p. 194-197.

Rowley, D.B., 2017. Earth's constant mean elevation: implication for long-term sea level controlled by oceanic lithosphere in a Pitman world, Journal of Geology, v. 125, p. 141-153.

Rowley, D.B., and Currie, 2006. Paleo-altimetry of the late Eocene to Miocene Lunpola basin, central Tibet, Nature, v. 439, p. 677-681.

Rowley, D.B., and Garzione, C.N., 2007. Stable isotope-based paleoaltimetry, Annual Review of Earth and Planetary Science, v. 35, p. 463-508.

Rowley, D.B., Pierrehumbert, R.T., Currie, and Currie, B.S., 2001. A new approach to stable isotope-based paleoaltimetry: implications for paleoaltimetry and paleohypsometry of the High Himalaya since the Late Miocene, Earth and Planetary Science Letters, v. 188, p.253-268.

Scotese, C.R., Phanerozoic plate tectonic reconstructions Atlas Scotese, C.R., 1990. Atlas of Phanerozoic Plate Tectonic Reconstructions, PALEOMAP Progress 01-1090a, Department of Geology, University of Texas at Arlington, Texas, 57 pp.

Scotese, C.R., 2001. Animation of Plate Motions and Global Plate Boundary Evolution since the Late Precambrian, Geological Society of America, 2001 Annual Meeting, Boston, (November 2–6), Abstracts with Programs, v. 33, issue 6, p.85.

Scotese, C.R., 2002. 3D paleogeographic and plate tectonic reconstructions: The PALEOMAP Project is back in town, presented at Houston Geological Society International Exploration Dinner Meeting, Houston, TX, May 20, 2002, The Bulletin of the Houston Geological Society, v. 44, issue 9, p. 13-15

Scotese, C.R., 2008a, The PALEOMAP Project PaleoAtlas for ArcGIS, version 1, Volume 1, Cenozoic Paleogeographic, Paleoclimatic and Plate Tectonic Reconstructions, PALEOMAP Project, Arlington, Texas.

Scotese, C.R., 2008b, The PALEOMAP Project PaleoAtlas for ArcGIS, version 1, Volume 2, Cretaceous Paleogeographic, Paleoclimatic, and Plate Tectonic Reconstructions, PALEOMAP Project, Arlington, Texas.

Scotese, C.R., 2008c, The PALEOMAP Project PaleoAtlas for ArcGIS, version 1, Volume 3, Triassic and Jurassic Paleogeographic, Paleoclimatic, and Plate Tectonic Reconstructions, PALEOMAP Project, Arlington, Texas.
Scotese, C.R., 2008d, The PALEOMAP Project PaleoAtlas for ArcGIS, v.1, Volume 4, Late Paleozoic Paleogeographic, Paleoclimatic, and Plate Tectonic Reconstructions, PALEOMAP Project, Arlington, Texas.
Scotese, C.R., 2008e, The PALEOMAP Project PaleoAtlas for ArcGIS, v.1, Volume 5, Early Paleozoic Paleogeographic, Paleoclimatic, and Plate Tectonic Reconstructions, PALEOMAP Project, Arlington, Texas.
Scotese, C.R., 2008f, The PALEOMAP Project PaleoAtlas for ArcGIS, v.1, Volume 6, Late Precambrian Paleogeographic, Paleoclimatic, and Plate Tectonic Reconstructions, PALEOMAP Project, Arlington, Texas.
Scotese, C.R, 2014a. Atlas of Phanerozoic Oceanic Anoxia (Mollweide Projection), Volumes 1-6, PALEOMAP Project PaleoAtlas for ArcGIS, PALEOMAP Project, Evanston, IL.
Scotese, C.R., 2014b. Atlas of Plate Tectonic Reconstructions (Mollweide Projection), Volumes 1-6, PALEOMAP Project PaleoAtlas for ArcGIS, PALEOMAP Project, Evanston, IL.
Scotese, C.R., 2014c. Atlas of Neogene Paleogeographic Maps (Mollweide Projection), Maps 1-7, Volume 1, The Cenozoic, PALEOMAP Atlas for ArcGIS, PALEOMAP Project, Evanston, IL. ResearchGate Academia
Scotese, C.R., 2014d. Atlas of Paleogene Paleogeographic Maps (Mollweide Projection), Maps 8-15, Volume 1, The Cenozoic, PALEOMAP Atlas for ArcGIS, PALEOMAP Project, Evanston, IL. ResearchGate Academia
Scotese, C.R., 2014e. Atlas of Late Cretaceous Paleogeographic Maps, PALEOMAP Atlas for ArcGIS, volume 2, The Cretaceous, Maps 16 ╨ 22, Mollweide Projection, PALEOMAP Project, Evanston, IL. ResearchGate Academia
Scotese, C.R., 2014f. Atlas of Early Cretaceous Paleogeographic Maps, PALEOMAP Atlas for ArcGIS, volume 2, The Cretaceous, Maps 23-31, Mollweide Projection, PALEOMAP Project, Evanston, IL. ResearchGate Academia
Scotese, C.R., 2014g. Atlas of Jurassic Paleogeographic Maps, PALEOMAP Atlas for ArcGIS, volume 3, The Jurassic and Triassic, Maps 32-42, Mollweide Projection, PALEOMAP Project, Evanston, IL. ResearchGate Academia
Scotese, C.R., 2014h. Atlas of Middle & Late Permian and Triassic Paleogeographic Maps, maps 43 - 48 from Volume 3 of the PALEOMAP Atlas for ArcGIS (Jurassic and Triassic) and maps 49 – 52 from Volume 4 of the PALEOMAP PaleoAtlas for ArcGIS (Late Paleozoic), Mollweide Projection, PALEOMAP Project, Evanston, IL. ResearchGate Academia
Scotese, C.R., 2014i. Atlas of Permo-Carboniferous Paleogeographic Maps (Mollweide Projection), Maps 53 – 64, Volume 4, The Late Paleozoic, PALEOMAP Atlas for ArcGIS, PALEOMAP Project, Evanston, IL.
Scotese, C.R., 2014j. Atlas of Devonian Paleogeographic Maps, PALEOMAP Atlas for ArcGIS, volume 4, The Late Paleozoic, Maps 65-72, Mollweide Projection, PALEOMAP Project, Evanston, IL. ResearchGate
Scotese, C.R., 2014k. Atlas of Silurian and Middle-Late Ordovician Paleogeographic Maps (Mollweide Projection), Maps 73 – 80, Volumes 5, The Early Paleozoic, PALEOMAP Atlas for ArcGIS, PALEOMAP Project, Evanston, IL. ResearchGate
Scotese, C.R., 2014l. Atlas of Cambrian and Early Ordovician Paleogeographic Maps (Mollweide Projection), Maps 81-88, Volumes 5, The Early Paleozoic, PALEOMAP Atlas for ArcGIS, PALEOMAP Project, Evanston, IL. ResearchGate
Scotese, C.R., 2014m. The PALEOMAP Project PaleoAtlas for ArcGIS, version 2, Volume 1, Cenozoic Paleogeographic and Plate Tectonic Reconstructions, Maps 1 – 15. PALEOMAP Project, Evanston, IL. DOI:10.13140/RG.2.1.2535.7041.
Scotese, C.R., 2014n. The PALEOMAP Project PaleoAtlas for ArcGIS, version 2, Volume 2, Cretaceous Paleogeographic and Plate Tectonic Reconstructions, Maps 16 – 31, PALEOMAP Project, Evanston, IL. DOI 10.13140/RG.2.1.2011.4162
Scotese, C.R., 2014o. The PALEOMAP Project PaleoAtlas for ArcGIS, version 2, Volume 3, Triassic and Jurassic Paleogeographic and Plate Tectonic Reconstructions, Maps 32 – 48, PALEOMAP Project, Evanston, IL. DOI 10.13140/RG.2.1.4108.5685
Scotese, C.R., 2014p. The PALEOMAP Project PaleoAtlas for ArcGIS, version 2, Volume 4, Late Paleozoic Paleogeographic and Plate Tectonic Reconstructions, Maps 49 – 72, PALEOMAP Project, Evanston, IL. DOI 10.13140/RG.2.1.2109.7206
Scotese, C.R., 2014q. The PALEOMAP Project PaleoAtlas for ArcGIS, version 2, Volume 5, Early Paleozoic Paleogeographic and Plate Tectonic Reconstructions, Maps 73 – 88, PALEOMAP Project, Evanston, IL. DOI 10.13140/RG.2.1.1585.4329
Scotese, C.R., 2014r. The PALEOMAP Project PaleoAtlas for ArcGIS, version 2, Volume 6, Late Precambrian Paleogeographic and Plate Tectonic Reconstructions, Maps 88 - 93, PALEOMAP Project, Evanston, IL. DOI 10.13140/RG.2.1.1323.2880
Scotese, C.R., 2015. The Ultimate Plate Tectonic Flipbook, Rob Van der Voo Retirement Symposium, Department of Earth and Environmental Sciences, University of Michigan, Ann Arbor, MI, August 26-27, 2015.
Scotese, C.R., 2016a. Continental Flooding & Orography, PALEOMAP Project, https://www.youtube.com/watch?v=y-Qh1Zp9WoM, DOI: 10.13140/RG.2.2.10331.36649, Evanston, IL.

Scotese, C. R., 2016b. Tutorial: PALEOMAP Paleoatlas for GPlates and the PaleoData Plotter Program, http://www.earthbyte.org/paleomap-paleoatlas-for-gplates/

Scotese, C.R., 2017. Atlas of Oceans & Continents: Plate Tectonics, 1.5 by – Today, PALEOMAP Project Report 112117A www.researchgate.net/publication/321197460 Atlas_of_Ancient_Oceans_Continents_15_billion_years_-_Today, 74 p.

Scotese, C.R., Boucot, A.J., and Chen, XU, 2014. Atlas of Phanerozoic Cimate Zones (Mollweide Projection), Volumes 1-6, PALEOMAP Project PaleoAtlas for ArcGIS, PALEOMAP Project, Evanston, IL.

Scotese, C.R., Dammrose, R., 2008. Plate Boundary Evolution and Mantle Plume Eruptions during the last Billion Years, Geological Society of America 2008 Annual Meeting, October 5-9, 2008, Houston, TX, Abstracts with Programs, v. 40, issue 6, Abstract 233-3, p. 328.

Scotese, C.R. and Elling, R., 2017. Plate Tectonic Evolution during the Last 1.3 Billion Years: The Movie, William Smith Meeting 2017: Plate Tectonics at 50. Geological Society of London, September 29 – October 1, 2017.

Scotese, C.R., Illich, H., Zumberge, J, and Brown, S., and Moore, T., 2007. The GANDOLPH Project: Year One Report: Paleogeographic and Paleoclimatic Controls on Hydrocarbon Source Rock Deposition, A Report on the Methods Employed, the Results of the Paleoclimate Simulations (FOAM), and Oils/Source Rock Compilation, Conclusions at the End of Year One: Cenomanian/Turonian (93.5 Ma), Kimmeridgian/Tithonian (151 Ma), Sakmarian/Artinskian (284 Ma), Frasnian/Famennian (375 Ma), February, 2007. GeoMark Research Ltd, Houston, Texas, 142 pp.

Scotese, C.R., Illich, H., Zumberge, J, and Brown, S., and Moore, T., 2008. The GANDOLPH Project: Year Two Report: Paleogeographic and Paleoclimatic Controls on Hydrocarbon Source Rock Deposition, A Report on the Methods Employed, the Results of the Paleoclimate Simulations (FOAM), and Oils/Source Rock Compilation, Conclusions at the End of Year Two: Miocene (10Ma), Aptian/Albian (120 Ma), Berriasian/Barremian (140 Ma), Late Triassic (220 Ma), and Early Silurian (430 Ma), July, 2008. GeoMark Research Ltd, Houston, Texas, 177 pp.

Scotese, C.R., Illich, H., Zumberge, J, and Brown, S., and Moore, T., 2009. The GANDOLPH Project: Year Three Report: Paleogeographic and Paleoclimatic Controls on Hydrocarbon Source Rock Deposition, A report on the Results of the Paleogeographic, Paleoclimatic Simulations (FOAM), and Oils/Source Rock Compilation, Conclusions at the End of Year Three: Eocene (45Ma), Early/Middle Jurassic (180 Ma), Mississippian (340 Ma), Neoproterozoic (600 Ma), August 2009, GeoMark Research Ltd, Houston, Texas, 154 pp.

Scotese, C.R., Illich, H., Zumberge, J, and Brown, S., and Moore, T., 2011. The GANDOLPH Project: Year Four Report: Paleogeographic and Paleoclimatic Controls on Hydrocarbon Source Rock Deposition, A report on the Results of the Paleogeographic, Paleoclimatic Simulations (FOAM), and Oils/Source Rock Compilation, Conclusions at the End of Year Four: Oligocene (30 Ma), Cretaceous/Tertiary (70 Ma), Permian/Triassic (250 Ma), Silurian/Devonian (400 Ma), Cambrian/Ordovician (480 Ma), April, 2011. GeoMark Research Ltd, Houston, Texas, 219 pp.

Scotese, C.R. and McKerrow, W.S., 1990. Revised world maps and introduction, in Paleozoic Paleogeography and Biogeography, W.S. McKerrow and C.R. Scotese (editors), Geological Society of London, Memoir 12, p. 1-21.

Scotese, C.R., and Moore, T.L., 2014a. Atlas of Phanerozoic Ocean Currents and Salinity (Mollweide Projection), Volumes 1-6, PALEOMAP Project PaleoAtlas for ArcGIS, PALEOMAP Project, Evanston, IL.

Scotese, C.R., and Moore, T.L., 2014b. Atlas of Phanerozoic Rainfall (Mollweide Projection), Volumes 1-6, PALEOMAP Project PaleoAtlas for ArcGIS, PALEOMAP Project, Evanston, IL.

Scotese, C.R., and Moore, T.L., 2014c. Atlas of Phanerozoic Temperatures (Mollweide Projection), Volumes 1-6, PALEOMAP Project PaleoAtlas for ArcGIS, PALEOMAP Project, Evanston, IL.

Scotese, C.R., and Moore, T.L., 2014d. Atlas of Phanerozoic Winds and Atmospheric Pressure (Mollweide Projection), Volumes 1-6, PALEOMAP Project PaleoAtlas for ArcGIS, PALEOMAP Project, Evanston, IL.

Scotese, C.R., and Moore, T.L., 2014e. Atlas of Phanerozoic Upwelling Zones (Mollweide Projection), Volumes 1-6, PALEOMAP Project PaleoAtlas for ArcGIS, PALEOMAP Project, Evanston, IL.

Scotese, C.R. and Sager, W.W., 1988. 8th Geodynamics Symposium, Mesozoic and Cenozoic Plate Reconstructions, Tectonophysics, v. 155, issues 1-4, p. 1-399.

Scotese, C.R., and Schettino, 2017. Late Permian – Early Jurassic Paleogeography of Western Tethys and the World, in Permo-Triassic Salt Provinces of Europe, North Africa and the Atlantic Margins, J.I. Soto, J. Flinch, & G. Tari (editors), Elsevier, pp. 57-95.

Smith, W.H.F., and Sandwell, D.T., 1997. Global Sea Floor Topography from Satellite Altimetry and Ship Depth Soundings, Science, v. 277, p. 1956-1962.

Smith, William, 1815. A Delineation of the Strata of England and Wales and part of Scotland, Geological Society of London.

Stein, C.A. and Stein, S. 1992. A model for the global variation in oceanic depth and heat flow with lithospheric age, Nature, v. 359, p. 123-129.

Verard, C., Hochard, C., Baumgartner, P.O., and Stampfli, G.M., 2015. 3D palaeogeographic reconstructions of the Phanerozoic versus sea-level and Sr- ratio variations. Journal of Palaeogeography, vol. 4, no. 1, p. 64-84.

Wright, N., Zahirovic, S., Müller, R.D., and Seton, M., 2013. Towards community-driven paleogeographic reconstructions: integrating open-access paleogeographic and paleobiology data with plate tectonics, Biogeosciences, 10, 1529-1541, https://doi.org/10.5194/bg-10-1529-2013.

Ziegler, A.M., 1975. A Proposal to Produce an Atlas of Paleogeographic Maps, Department of Geophysical Sciences, University of Chicago, 17 pp.

Ziegler, A.M., and Scotese, 1977. Thoughts on Format for the Forthcoming “Atlas of Paleogeographic Maps”, Department of Geophysical Sciences, University of Chicago, 6 pp.

Ziegler, A.M., Rowley, D.B., Lottes, A.L., Sahagian, D.L., Hulver, M.L., and Gierlowski, T.C., 1985. Paleogeographic interpretation: With an Example from the Mid-Cretaceous, Annual Review of Earth Sciences, volume 13, p. 385-425.

List of Tables

List of Figures

Table 1. List of Time Intervals for PaleoDEMs (**bold** = original paleoDEMS)

Number	Stratigraphic Age	Plate Tectonic Model Age[3]
1	**Present-day (Holocene, 0 Ma)**	**0**
2	**Last Glacial Maximum (Pleistocene, 21 ky)[1]**	**0**
2.1	Late Pleistocene (122 ky)[1]	0
2.2	Middle Pleistocene (454 ky)[1]	0
2.3	Early Pleistocene (Calabrian, 1.29 Ma)[1]	0
2.4	Early Pleistocene (Gelasian, 2.19)[1]	0
2.5	Late Pliocene (Piacenzian, 3.09)[2]	5
3	Early Pliocene (Zanclean, 4.47 Ma)	5
4	latest Miocene (Messinian, 6.3 Ma)[2]	5
5	**Middle/Late Miocene (Serravallian&Tortonian, 10.5 Ma)**	**10**
6	Middle Miocene (Langhian, 14.9 Ma)	15
7	**Early Miocene (Aquitanian&Burdigalian, 19.5 Ma)**	**20**
8	Late Oligocene (Chattian, 25.6 Ma)	25
9	**Early Oligocene (Rupelian, 31 Ma)**	**30**
10	Late Eocene (Priabonian, 35.9 Ma)	35
11	**late Middle Eocene (Bartonian, 39.5 Ma)**	**40**
12	early Middle Eocene (Lutetian, 44.5 Ma)	45
13	**Early Eocene (Ypresian, 51.9 Ma)**	**50**
14	**Paleocene/Eocene Boundary (PETM, 56 Ma)**	**55**
15	**Paleocene (Danian&Thanetian, 61 Ma)**	**60**
16	KT Boundary (latest Maastrichtian, 66 Ma)	65
17	**Late Cretaceous (Maastrichtian, 69 Ma)**	**70**
18	Late Cretaceous (Late Campanian, 75 Ma)	75
19	**Late Cretaceous (Early Campanian, 80.8 Ma)**	**80**
20	Late Cretaceous (Santonian&Coniacian, 86.7 Ma)	85
21	**Mid-Cretaceous (Turonian , 91.9 Ma)**	**90**
22	Mid-Cretaceous (Cenomanian, 97.2 Ma)	95
23	**Early Cretaceous (late Albian, 102.6 Ma)**	**100**
24	Early Cretaceous (middle Albian, 107 Ma)	105
25	**Early Cretaceous (early Albian, 111 Ma)**	**110**
26	Early Cretaceous (late Aptian, 115.8 Ma)	115
27	**Early Cretaceous (early Aptian, 121.8 Ma)**	**120**
28	Early Cretaceous (Barremian, 127.2 Ma)	125
29	**Early Cretaceous (Hauterivian, 131.2 Ma)**	**130**
30	Early Cretaceous (Valanginian, 136.4 Ma)	135

31	**Early Cretaceous (Berriasian, 142.4 Ma)**	**140**
32	Jurassic/Cretaceous Boundary (145 Ma)	145
33	**Late Jurassic (Tithonian, 148.6 Ma)**	**150**
34	Late Jurassic (Kimmeridgian, 154.7 Ma)	155
35	**Late Jurassic (Oxfordian, 160.4 Ma)**	**160**
36	Middle Jurassic (Callovian, 164.8 Ma)	165
37	**Middle Jurassic (Bajocian&Bathonian, 168.2)**	**170**
38	Middle Jurassic (Aalenian, 172.2 Ma)	175
39	**Early Jurassic (Toarcian, 178.4 Ma)**	**180**
40	Early Jurassic (Pliensbachian, 186.8 Ma)	185
41	**Early Jurassic (Sinemurian/Pliensbachian, 190.8 Ma)**	**190**
42	Early Jurassic (Hettangian&Sinemurian, 196 Ma)	195
43	**Late Triassic (Rhaetian/Hettangian, 201.3 Ma)**	**200**
43.5	Late Triassic (Rhaetian, 204.9 Ma)	205
44	Late Triassic (late Norian, 213.2 Ma)	210
44.5	Late Triassic (mid Norian, 217.8 Ma)	215
45	**Late Triassic (early Norian, 222.4 Ma)**	**220**
45.5	Late Triassic (Carnian/Norian 227 Ma)	225
46	Late Triassic (Carnian, 232 Ma)	230
46.5	Late Triassic (early Carnian, 233.6)	235
47	**Middle Triassic (Ladinian, 239.5 Ma)**	**240**
48	Middle Triassic (Anisian, 244.6 Ma)	245
49	**Permo-Triassic Boundary (252 Ma)**	**250**
50	Late Permian (Lopingian, 256 Ma)	255
51	**late Middle Permian (Capitanian, 262.5 Ma)**	**260**
51.5	Middle Permian (Wordian/Capitanian Boundary 265.1 Ma)	265
52	Middle Permian (Roadian&Wordian, 268.7 Ma)	270
53	Early Permian (late Kungurian, 275 Ma)	275
54	**Early Permian (early Kungurian, 280 Ma)**	**280**
54.5	Early Permian (Artinskian, 286.8 Ma)	285
55	Early Permian (Sakmarian, 292.6 Ma)	290
56	Early Permian (Asselian, 297 Ma)	295
57	**Late Pennsylvanian (Gzhelian, 301.3 Ma)**	**300**
58	Late Pennsylvanian (Kasimovian, 305.4 Ma)	305
59	Middle Pennsylvanian (Moscovian, 311.1 Ma)	310
60	Early/Middle Carboniferous (Baskirian/Moscovian boundary, 314.6 Ma)	315
61	**Early Pennsylvanian (Bashkirian, 319.2 Ma)**	**320**
61.5	Late Mississippian (Serpukhovian, 327 Ma)	325
62	Late Mississippian (Visean/Serpukhovian boundary, 330.9 Ma)	330
62.5	Middle Mississippian (late Visean, 333 Ma)	335
63	**Middle Mississippian (middle Visean, 338.8Ma)**	**340**

63.5	Middle Mississippian (early Visean, 344 Ma)	345
64	Early Mississippian (late Tournaisian, 349 Ma)	350
64.5	Early Mississippian (early Tournaisian, 354Ma)	355
65	**Devono-Carboniferous Boundary (358.9 Ma)**	**360**
65.5	Late Devonian (middle Famennian, 365.6 Ma)	365
66	Late Devonian (early Famennian, 370 Ma)	370
66.5	Late Devonian (late Frasnian, 375 Ma)	375
67	**Late Devonian (early Frasnian, 380 Ma)**	**380**
67.5	Middle Devonian (Givetian, 385.2 Ma)	385
68	Middle Devonian (Eifelian, 390.5 Ma)	390
69	Early Devonian (late Emsian, 395 Ma)	395
70	**Early Devonian (middle Emsian, 400 Ma)**	**400**
70.5	Early Devonian (early Emsian, 405 Ma)	405
71	Early Devonian (Pragian, 409.2 Ma)	410
72	Early Devonian (Lochkovian, 415 Ma)	415
73	**Late Silurian (Pridoli, 421.1 Ma)**	**420**
74	Late Silurian (Ludlow, 425.2 Ma)	425
75	**Middle Silurian (Wenlock, 430.4 Ma)**	**430**
75.5	Early Silurian (late Llandovery, 436 Ma)	435
76	**Early Silurian (early Llandovery, 441.2 Ma)**	**440**
77	Late Ordovician (Hirnantian, 444.5 Ma)	445
78	Late Ordovician (Katian, 449.1 Ma)	450
79	Late Ordovician (Sandbian, 455.7 Ma)	455
80	**Middle Ordovician (late Darwillian,460 Ma)**	**460**
80.5	Middle Ordovician (early Darwillian,465 Ma)	465
81	Early Ordovician (Floian/Dapingianboundary, 470 Ma)	470
81.5	Early Ordovician (late Early Floian, 475 Ma)	475
82	**Early Ordovician (Tremadoc, 481.6 Ma)**	**480**
82.5	Cambro-Ordovician Boundary (485.4 Ma)	485
83	Late Cambrian (Jiangshanian, 491.8 Ma)	490
83.5	Late Cambrian (Pabian, 495.5 Ma)	495
84	**late Middle Cambrian (Guzhangian, 498.8 Ma)**	**500**
84.1	late Middle Cambrian (early Epoch 3, 505 Ma)	505
84.2	early Middle Cambrian (late Epoch 2, 510 Ma)	510
85	early Middle Cambrian (middle Epoch 2, 515 Ma)	515
86	**Early/Middle Cambrian boundary (520 Ma)**	**520**
86.5	Early Cambrian (late Terreneuvian, 525 Ma)	525
87	Early Cambrian (middle Terreneuvian, 530 Ma)	530
87.5	Early Cambrian (early Terreneuvian, 535 Ma)	535
88	**Cambrian/Precambrian boundary (541 Ma)**	**540**
89	Late Neoproterozoic (late Ediacaran, 560 Ma)	560

89.1	Late Neoproterozoic (late Ediacaran, 570 Ma)	570
90	**Late Neoproterozoic (middle Ediacaran, 600 Ma)**	**600**
91	Late Neoproterozoic (early Ediacaran, 650 Ma)	660
92	**Middle Neoproterozoic (late Cryogenian, 690 Ma)**	**690**
93	Middle Neoproterozoic (early Cryogenian, 700 Ma)	700
94	**Early Neoproterozoic (late Tonian. 750 Ma)**	**750**
95	Early Neoproterozoic (middle Tonian, 800 Ma)	800
96	Early Neoproterozoic (middle Tonian, 850 Ma)	850
97	Early Neoproterozoic (early Tonian, 900 Ma)	900
98	Early Neoproterozoic (early Tonian, 950 Ma)	950
99	Mesoproterozoic / Neoproterozoic Boundary (1000 Ma)	1000
100	Late Mesoproterozoic (late Stenian, 1050 Ma)	1050
100	Late Mesoproterozoic (middle Stenian, 1100 Ma)	1100
101	Late Mesoproterozoic (early Stenian, 1150 Ma)	1150
102	Late/Middle Mesoproterozoic Boundary (1200 Ma)	1200
103	Middle Mesoproterozoic (late Ectesian, 1250 Ma)	1250
104	Middle Mesoproterozoic (middle Ectasian, 1300 Ma)	1300
105	Middle Mesoproterozoic (early Ectasian, 1350 Ma)	1350
106	Middle/Early Mesoproterozoic Boundary (1400 Ma)	1400
107	Early Mesoproterozoic (late Calmmian, 1450 Ma)	1450
108	Early Mesoproterozoic (middle Calymmian, 1500 Ma)	1500
109	Late Paleoproterozoic (Statherian, 1700 Ma)	1700
110	Middle Paleoproterozoic (Orosirian, 1900 Ma)	1900
111	Middle PaleoProterozoic (Rhyacian, 2100 Ma)	2100
112	Early Paleoproterozoic (Siderian, 2500 Ma)	2500
113	Archean (Neoarchean, 2650 Ma)	2650
114	Archean (Mesoarchean, 3000 Ma)	3000
115	Archean (Paleoarchean, 3400 Ma)	3400
116	Archean (Eoarchean, 3800 Ma)	3800
117	Hadean (4600 - 4000 Ma)	4300

Explanation: Stratigraphic age in millions of years from Ogg, Ogg, & Gradstein (2012). Bold Text: original maps, Scotese (2008a-f). All other maps are from Scotese (2014a-f). Grayed out intervals are currently not available as PALEOMAP PaleoDEMS. 1 – Pleistocene maps use modern base map. 2 – All Pliocene maps use the 5 Ma reconstruction. 3 - “Plate Tectonic Model Age” refers to the corresponding age in the PALEOMAP Global Plate Model v2d3 (Scotese, 2016b). Use the “Plate Tectonic Model Age” when producing plate tectonic basemaps in GPlates.

Table 2. Elevation ranges of environments shown on paleogeographic maps

Code	Elevation	Environments	Geological Evidence
9	10,000 to 4000 m	Collisional mountains	High-T, high-P metamorphics
8	4000 to 2000 m	Andean-type mountains	Andesites/granodiorites in a continental setting
7	2000 to 1000 m	a. Island arc volcanos	Andesites/granodiorites in a marine setting
		b. Intra-continental rift shoulders	Adjacent fanglomerates
6	1000 to 200m	a. Rift valley	Basalts, lake deposits in grabens
		b. Some forearc ridges	Tectonic mélanges
5	200m to Sea Level	a. Coastal plains	Alluvial complexes
		b. Lower river systems	Major floodplain complexes
		c. Delta tops	Swamps and channel sands
4	Sea Level to -50 m	a. Inner shelves	Heterogeneous marine sediments
		b. Reef-dammed shelves	Bahamian-type carbonates
		c. Delta fronts	Topset silts and sands
3	-50 to -200 m	a. Outer shelves	Fine sediments, most bioproductites
		b. Some epeiric basins	Fine clastics or carbonates
		c. Pro-deltas	Foreset silts and proximal turbidites
2	-200 to -4000 m	a. Continental slope/rise	Slump/contourite facies
		b. Mid-ocean ridges	Oceanic crust less than 60 m.y. old
		c. Pro-delta fans	Bottomset clays and distal turbidites
1	-4000 to -6000 m	Ocean floors	Pelagic sequences on oceanic crust
0	-6000 to -12000 m	Ocean trenches	Turbidites on pelagic sequences

from Ziegler et al., 1985

Table 3. Legend for Lithofacies Symbols (See Figure 5)

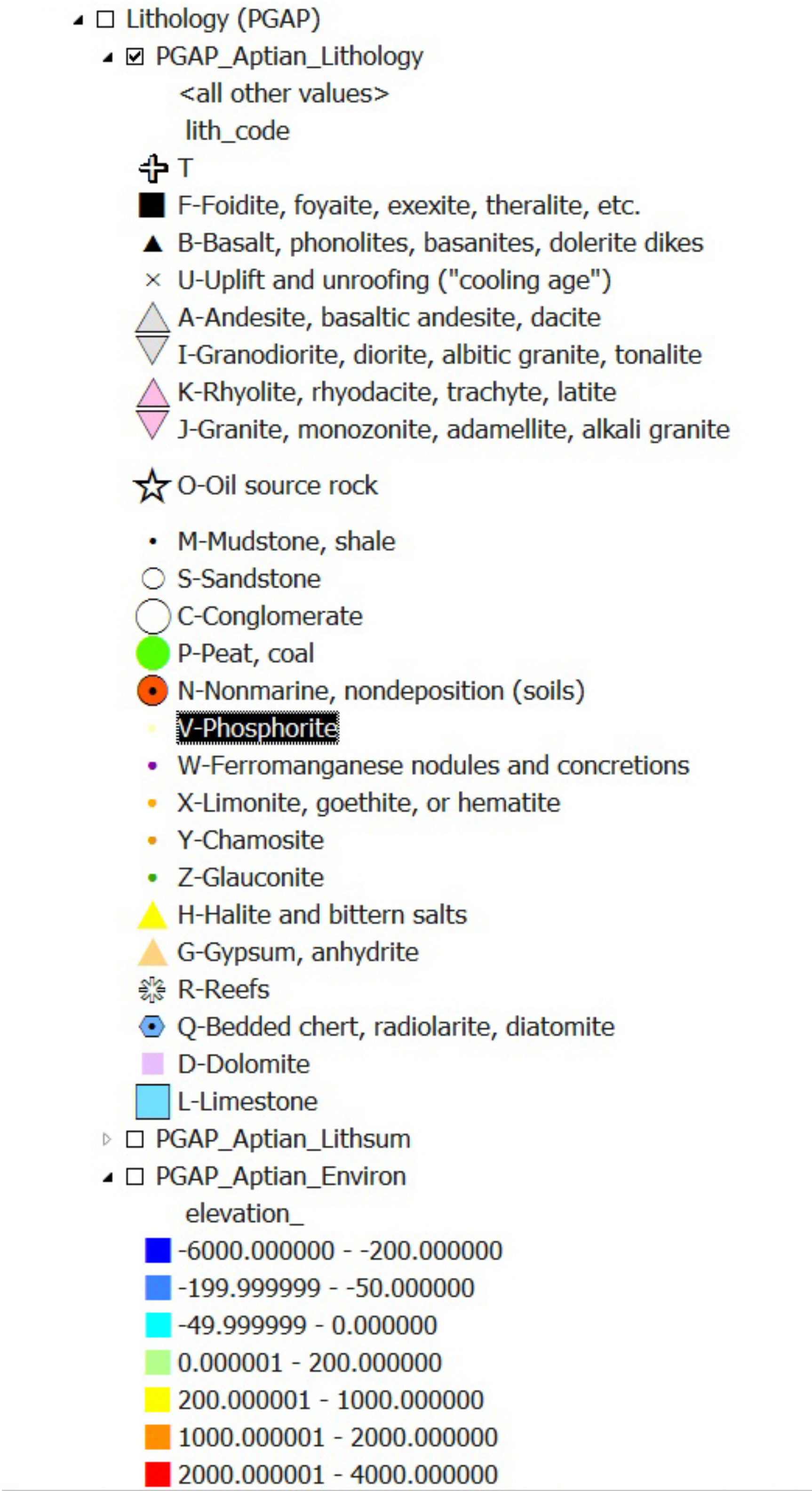

- Lithology (PGAP)
  - PGAP_Aptian_Lithology
    - <all other values>
    - lith_code
    - T
    - F-Foidite, foyaite, exexite, theralite, etc.
    - B-Basalt, phonolites, basanites, dolerite dikes
    - U-Uplift and unroofing ("cooling age")
    - A-Andesite, basaltic andesite, dacite
    - I-Granodiorite, diorite, albitic granite, tonalite
    - K-Rhyolite, rhyodacite, trachyte, latite
    - J-Granite, monozonite, adamellite, alkali granite
    - O-Oil source rock
    - M-Mudstone, shale
    - S-Sandstone
    - C-Conglomerate
    - P-Peat, coal
    - N-Nonmarine, nondeposition (soils)
    - V-Phosphorite
    - W-Ferromanganese nodules and concretions
    - X-Limonite, goethite, or hematite
    - Y-Chamosite
    - Z-Glauconite
    - H-Halite and bittern salts
    - G-Gypsum, anhydrite
    - R-Reefs
    - Q-Bedded chert, radiolarite, diatomite
    - D-Dolomite
    - L-Limestone
  - PGAP_Aptian_Lithsum
  - PGAP_Aptian_Environ
    - elevation_
    - -6000.000000 - -200.000000
    - -199.999999 - -50.000000
    - -49.999999 - 0.000000
    - 0.000001 - 200.000000
    - 200.000001 - 1000.000000
    - 1000.000001 - 2000.000000
    - 2000.000001 - 4000.000000

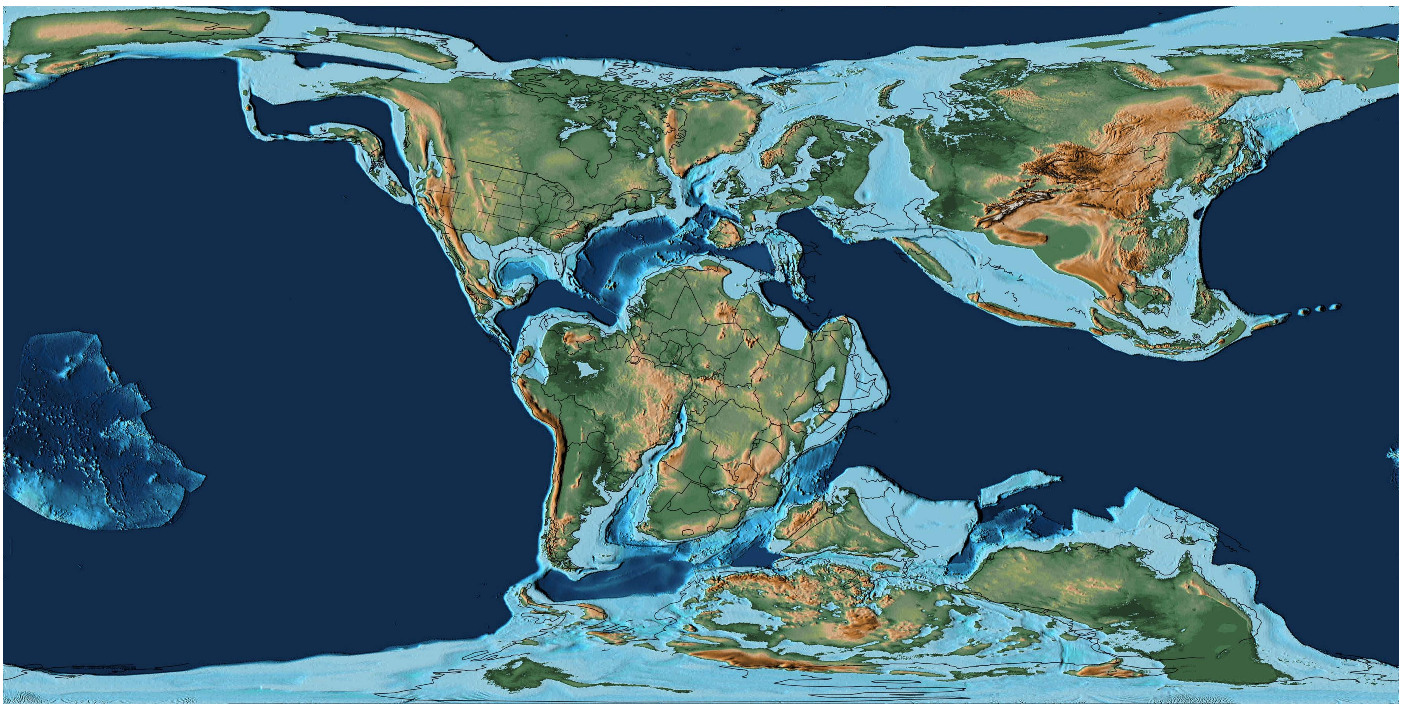

Figure 1. Paleogeographic Map for the Early Cretaceous (Early Aptian, 121.8 Ma; Rectilinear Projection)

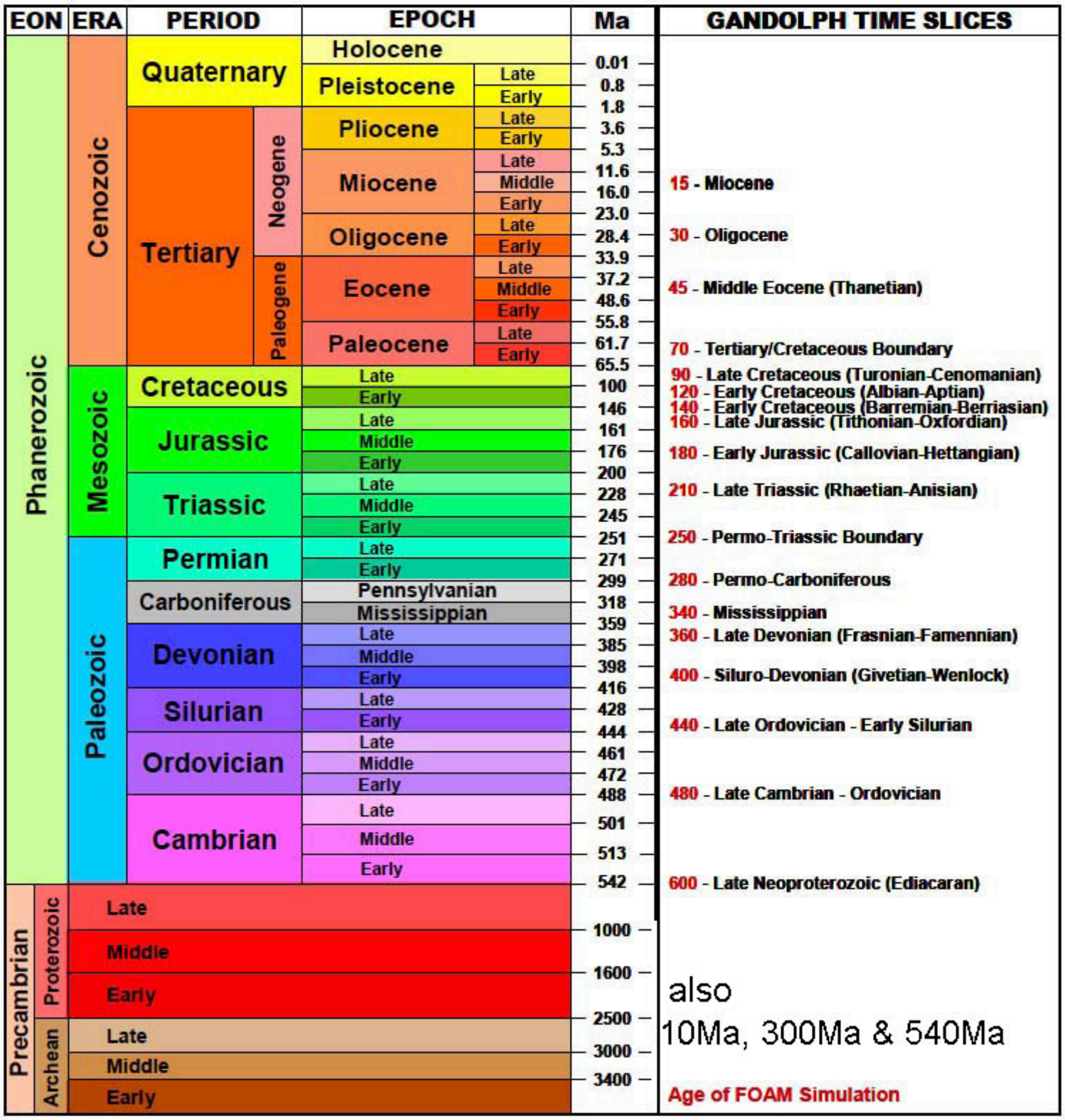

Figure 2. Time Intervals of FOAM Paleoclimate Simulations

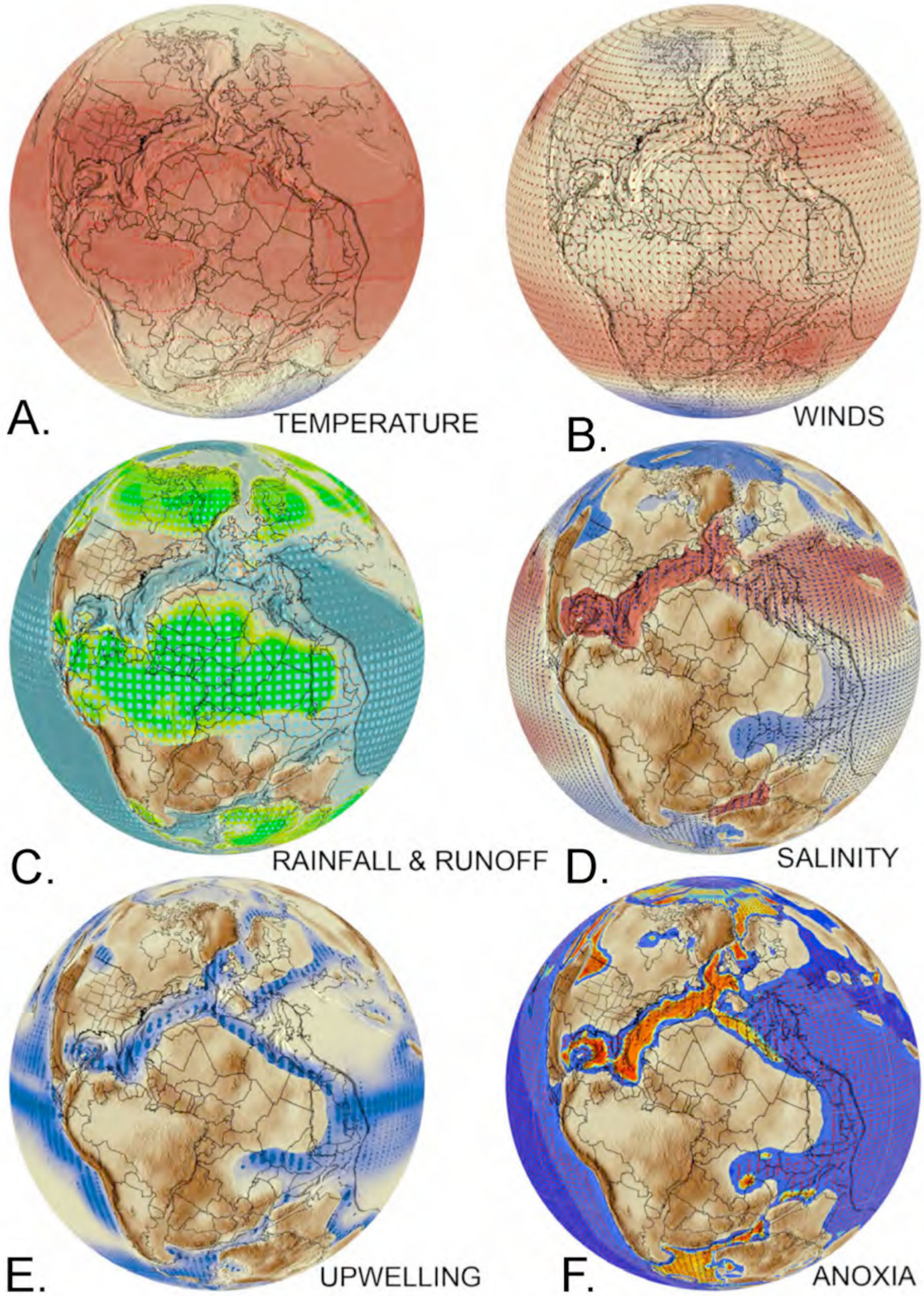

Figure 3. Example Output from FOAM Paleoclimate Simulations Using PALEOMAP PaleoDEMs

LEGEND

Paleogeography - ocean basin (blue), shallow sea (light blue), land (green), uplands (brown)

Upwelling – zones of upwelling are indicated by blue shading; the size of the blue dots is proportional to the volume and persistence of the upwelling zone

Restriction – “restricted” regions: location of areas with limited connections to the open ocean (red – more restricted, blue – less restricted); summer ocean surface currents (red arrows)

Salinity – salinity of the surface waters of the deep ocean and shallow seas (red – hypersaline, blue – brackish); blue arrows indicate the direction of oceanic circulation (surface waters)

High/Low Stand – relative proportions of flooded continental areas during highstands (blue dashed line) and lowstands (brown dashed line)

Rainfall – annual average rainfall (blue squares) and surface runoff (green shading)

Rivers – river systems (size of blue triangles proportional to river volume) and deltas (black circles with green plus sign)

Summer Winds – wind direction (red arrows), high atmospheric sea level pressure (red), low atmospheric pressure (blue/yellow)

Winter Winds – wind direction (blue arrows), high atmospheric sea level pressure (red), low atmospheric pressure (blue/yellow)

Summer Temperature – global surface temperature with isotherms (°C) during the northern hemisphere winter

Winter Temperature – global surface temperature with isotherms (°C) during the northern hemisphere summer

On all Maps – source rock localities; basins with source rocks (red shading)

Figure 4. Legend for FOAM Paleoclimate Simulations (Scotese et al., 2007, 2008, 2009, 2011)

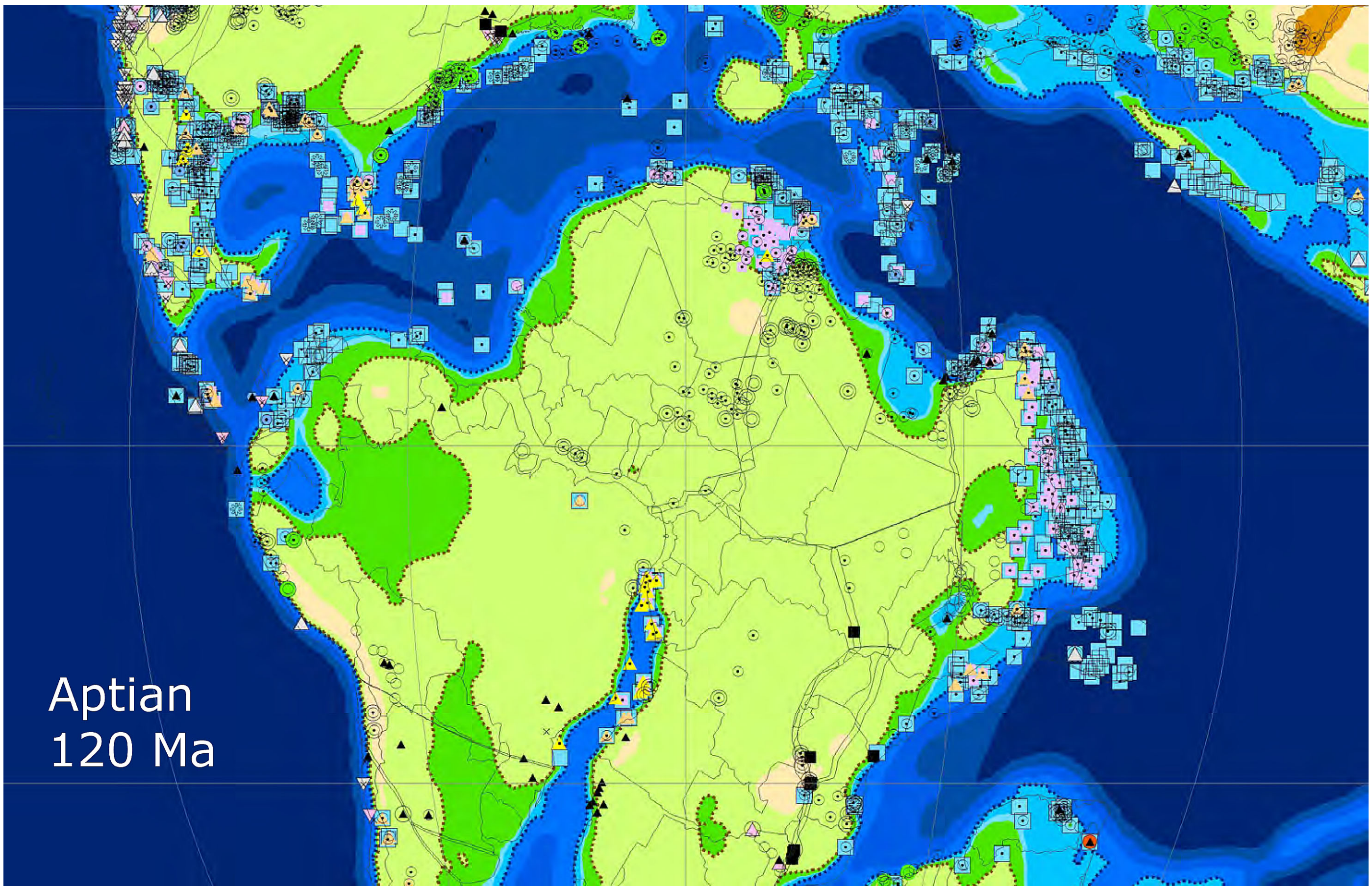

Figure 5. Lithofacies Used to Map Paleogeography (for explanation of symbols see Table 3.)

Figure 6. Color Codes for Paleotopography and Paleobathymetry

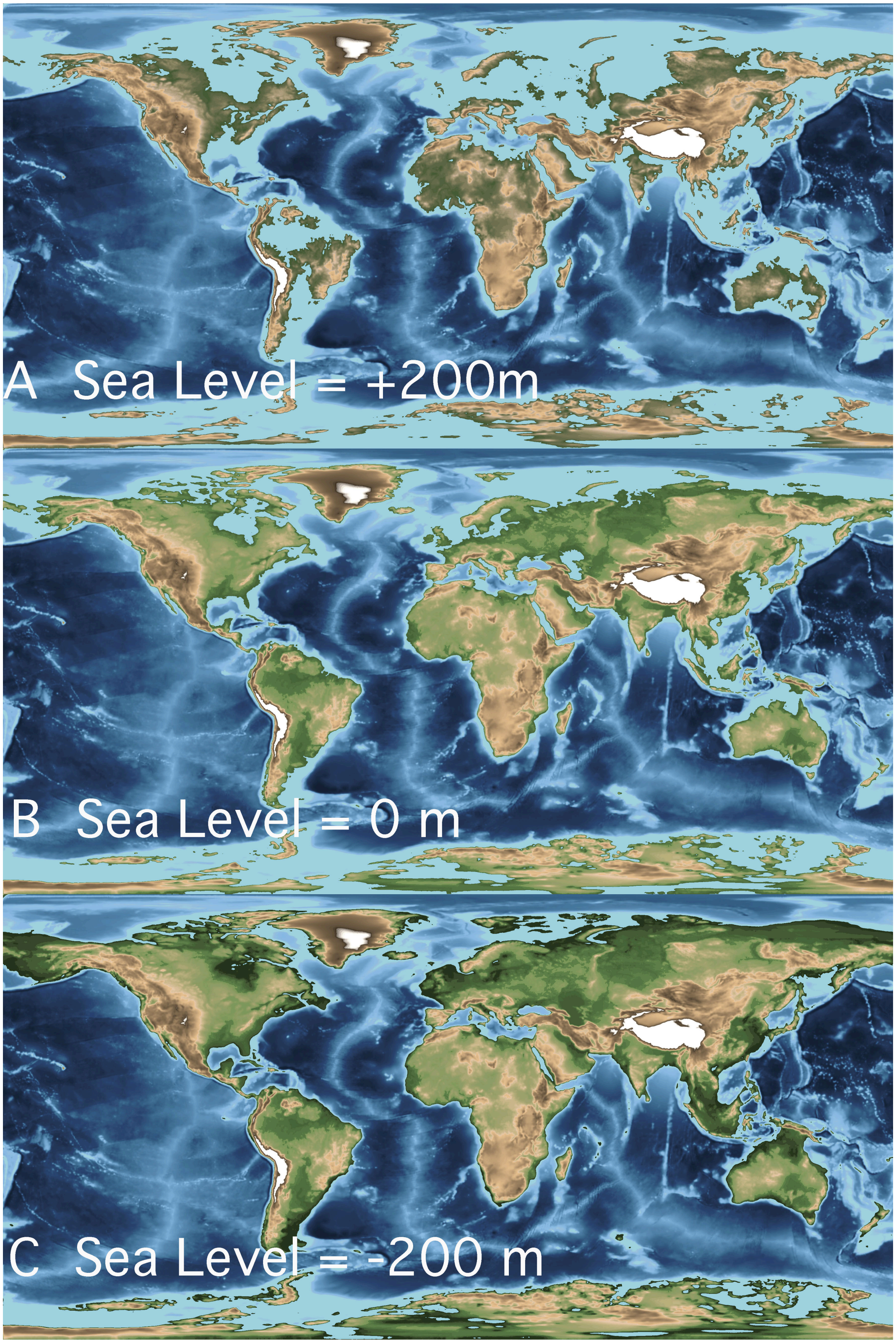

Figure 7. A. Modern PaleoDEM with sea level raised +200 m, B. Modern PaleoDEM with Sea Level = 0 m, Modern PaleoDEM with sea level dropped -200 m.